

Vehicle Collision with Bridge Piers

Sherif El-Tawil, P.E., M.ASCE¹; Edward Severino²; and Priscilla Fonseca³

Abstract: Inelastic transient finite element simulations are used to investigate the demands generated during collisions between vehicles and bridge piers. Such collisions have occurred in the past, sometimes with catastrophic consequences. Two different types of trucks and two different bridge/pier systems are used in the simulations. The approach speeds for the trucks range from 55 to 135 kph. Various quantities of interest are extracted from the finite element results and used to develop a better understanding of the vehicle/pier crash process and to critique current specifications addressing such events. Although physical vehicle–pier impact tests were not carried out as part of this research, a variety of exercises are conducted to provide confidence in the analysis results. The simulations show that current collision design provisions could be unconservative and that there may be a population of bridge piers that are vulnerable to accidental or malicious impact by heavy trucks.

DOI: 10.1061/(ASCE)1084-0702(2005)10:3(345)

CE Database subject headings: Collisions; Vehicles; Bridges, piers; Finite elements; Simulations; Traffic accidents.

Introduction

Accidental collisions of heavy vehicles with bridge piers have occurred in the past, sometimes with catastrophic consequences. The writers have documented three events that have led to loss of life and complete destruction of the impacted bridge. Two of these events are quite recent.

1. At 1:35 a.m. on May 19, 1993, a tractor with a bulk-cement-tank semitrailer was driving south on I-65 near Evergreen, Ala., when it left the paved road, traveled over the embankment, overran a guardrail, and collided with a supporting bridge column of the County Road 22 overpass (NTSB 1993). Two spans of the overpass collapsed onto the semitrailer and southbound lanes of the interstate. An automobile and another tractor-semitrailer then collided with the collapsed bridge spans killing both drivers.
2. At 10:15 a.m. on September 9, 2002, a tractor-trailer going northbound on I-45 in Texas veered toward the southbound lanes and hit a concrete support column for the Highway 14 overpass, causing the bridge to collapse and killing one person (Dallas-News 2002).
3. At 9:00 p.m. on May 23, 2003, a semitrailer crashed into the median support of a bridge crossing I-80 near Big Springs, Neb., causing the overpass to collapse. Fig. 1 shows the collapsed bridge shortly after impact. One person was killed in the incident, and Memorial Day traffic was severely disrupted on the busy I-80 route (“Nebraska” 2003).

To cater for such events, the AASHTO-LRFD (1998) code has design criteria addressing vehicle collision. The provisions specify that bridge piers should be designed for a collision force—represented by an 1,800-kN static force—if they are not protected by a crashworthy barrier and are located within a distance of 10 m to the edge of a roadway. The force is applied in a horizontal plane located 1.35 m above ground and should be applied to the pier in the most critical direction. The commentary is rather vague about the origins of the provisions and states that the equivalent static force is based on information resulting from early full-scale crash tests of barriers for redirecting tractor-trailers and from analysis of other truck collisions. It does not indicate that the design forces were derived directly from head-on collision tests.

The AASHTO-LRFD (1998) vehicle collision provisions do not address several important issues. The design collision force is not specified as a function of the design speed of the adjacent roadway nor the vehicle characteristics. The dynamic interaction between the colliding vehicle and bridge structure is not recognized, nor indeed, even mentioned. It is well known that the failure mode under dynamic loading can be substantially different than under static loading. For instance, Miyamoto et al. (1994) document tests where reinforced concrete beams failed in flexure under static loading and by shear when subjected to impact loading. There are also no guidelines on how to detail a vulnerable member to ensure that it will survive (with a specific structural performance in mind) a catastrophic impact situation.

The accident reports for the three events described above indicate that the destroyed piers were protected by guard rails; see, for example, Fig. 1. However, it is unclear if the bridge designers had accounted for the possibility of impact in designing the piers, or whether they had relied on the guardrails to protect the bridge supports. It is also not known if the rails satisfy current guidelines for crashworthiness; they were certainly ineffective in protecting the piers and preventing loss of life. In spite of the potential inadequacy of guardrails under such severe crash conditions, it is nevertheless disturbing that some vulnerable bridges are not protected by guardrails at all as shown in Figs. 2(a and b). Given the exposure of protected and unprotected bridge piers to accidental or malevolent impact by heavy vehicles, there is an urgent need to

¹Associate Professor, Dept. of Civil and Environmental Engineering, Univ. of Michigan, Ann Arbor, MI 48109-2125.

²Bridge Design Engineer, HNTB, Orlando, FL 32822.

³Research Assistant, Dept. of Civil and Environmental Engineering, Univ. of Michigan, Ann Arbor, MI 48109-2125.

Note. Discussion open until October 1, 2005. Separate discussions must be submitted for individual papers. To extend the closing date by one month, a written request must be filed with the ASCE Managing Editor. The manuscript for this paper was submitted for review and possible publication on August 13, 2003; approved on May 4, 2004. This paper is part of the *Journal of Bridge Engineering*, Vol. 10, No. 3, May 1, 2005. ©ASCE, ISSN 1084-0702/2005/3-345-353/\$25.00.



Fig. 1. Collapse of I-80, Nebraska, bridge after being struck by tractor-trailer (courtesy of NDOR)

investigate the vehicle/pier collision process with the purpose of evaluating and eventually updating current guidelines.

This paper addresses this issue and presents the results of detailed finite element analyses of various vehicle/pier crash scenarios. Guardrails are not modeled in order to focus attention purely on vehicle/pier interaction. The resulting data is used to better understand the collision process and to critique current AASHTO-LRFD vehicle collision provisions.

Vehicle Models

Two publicly available vehicle finite element models are used to investigate structural demands imposed on bridge piers during vehicle/pier collision. The vehicle models are a 14-kN Chevy truck [Fig. 3(a)] and a 66-kN Ford truck [Fig. 3(b)]. The models were downloaded from the National Crash Analysis Center website (www.ncac.gwu.edu) at George Washington University. The Chevy model is the C-2500 “reduced” model, which has far fewer elements (10,650 elements) than the “detailed” model (with

54,800 elements) that is posted on the same website. The Ford model has 21,400 elements. The 14-kN Chevy truck is intended to represent light trucks, while the 66-kN Ford truck represents medium weight trucks. Models of heavier trucks are not yet available, although a 360-kN tractor-trailer model is currently under development at the US Federal Highway Administration.

These vehicle models and others like them were developed and validated by the Federal Government to be used in crashworthiness exercises and studies such as the one presented herein. The models were created through a painstaking process, whereby the geometry of various parts of each vehicle was digitized and imported into finite element modeling software. Coupons taken from the vehicle parts were tested to provide data for constitutive modeling. Several material models are used to represent the trucks including: (1) elastic material behavior is assumed for the engine, transmission, and radiator; (2) a rubber model is used for the mounts between the cabin and rails, engine and rails, and other mounts; (3) rigid material behavior is assigned to certain members connecting different components; and (4) rate-dependent isotropic elastic-plastic material model is used to represent the inelastic response of structural elements such as the chassis components and the body sheet metal. Different model parts are represented using shell, solid, or beam elements and are connected using various types of constraints that allow the vehicle components to interact together in a realistic manner. Further details about the Chevy model can be found in Zaouk et al. (1996).

Pier Models

Two pier models with different geometric characteristics and heights are used in the investigation. Pier dimensions were obtained from structural plans of existing vulnerable bridges in Florida. The first pier, hereafter referred to as Pier I, is a reinforced concrete column that has a 1,450 mm \times 1,375 mm cross section and is 16,300 mm high. The pier is attached to a reinforced concrete pile cap with dimensions 5,000 mm \times 4,000 mm \times 1,670 mm that is embedded 2,150 mm underground. The superstructure, pier, and cap are supported by twelve 450 mm diameter prestressed concrete piles 10,000 mm in length. Pier II is also a reinforced concrete pier. It has a circular cross



(a) Box girder bridge on single pier supports



(b) I-girder bridge on single pier supports

Fig. 2. Bridge piers vulnerable to impact by heavy vehicles

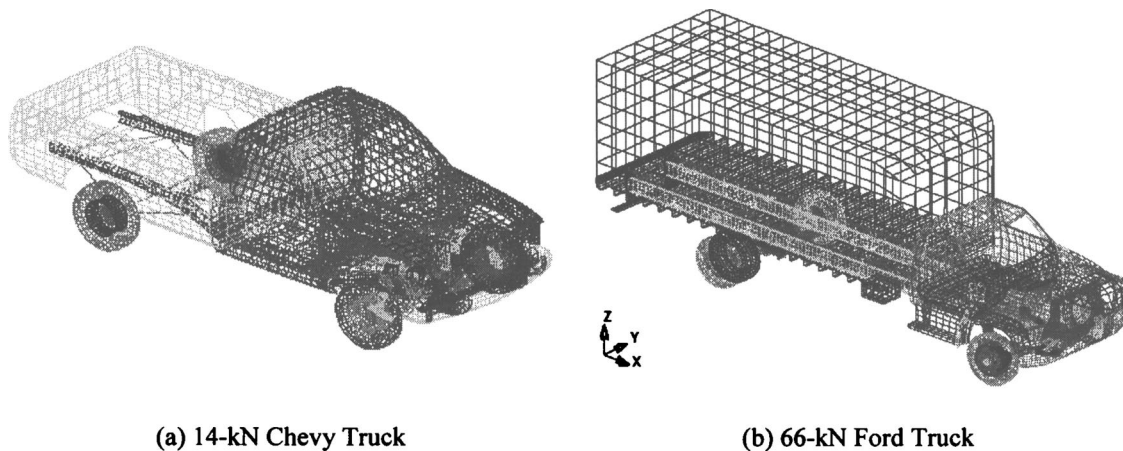


Fig. 3. Vehicle finite element models

section of 1,075 mm diameter and a height of 9,925 mm. It is attached to a reinforced concrete pile cap that is 3,300 mm \times 2,300 mm \times 1,075 mm in dimension and embedded 830 mm into the ground. The pile cap is supported on six 450 mm diameter prestressed concrete piles 10,000 mm in length. Pier I is reinforced with 24 No. 11 bars (35 mm diameter) and No. 5 (16 mm diameter) stirrups with four legs. Pier II has 14 No. 11 bars (35 mm diameter) and No. 5 (16 mm diameter) round hoops. Concrete in both piers is assumed to have a nominal strength of 23 MPa; steel is taken to have a yield strength of 400 MPa. The pier and pile cap are represented using fully integrated 8-node brick elements with elastic properties representing uncracked concrete.

The superstructure is modeled using beam elements. The dimensions and properties of the superstructure are obtained from the same structural plans from which Pier I details were derived. The same superstructure is used with both piers for simplicity, and is comprised of two adjacent composite steel-concrete box girders. The geometric properties of each box girder are as follows: area=80,133.0 mm², $I_{zz}=2.798\text{E}+10$ mm⁴, and $I_{yy}=8.340\text{E}+10$ mm⁴, where z =horizontal axis and y =vertical axis. In calculating these properties, the composite section is transformed into an equivalent steel section. The superstructure consists of two unequal spans of 53,400 and 50,000 mm, respectively, which are assumed to be pinned at their far ends. Each girder is modeled using 18 elastic beam elements, and its mass is assumed lumped at the beam nodes.

The superstructure transmits its weight to the piers through elastomeric bearing pads. Each girder is assumed to rest on two 200 mm \times 200 mm pads with four steel layers with a total thickness of 37 mm. Bearing pad properties were derived from tests reported in NCHRP Report 298 (Roeder et al. 1987). The bearings are represented by standard beam elements, whose flexural stiffness is adjusted to provide the same tip displacement as a shear flexible beam element with shear modulus $G=0.608$ MPa. It was not necessary to be more precise in modeling the bearing pads because sensitivity studies showed that the effect of bearing pad stiffness is almost insignificant. Analyses with 0.5, 2, and 4 times the assumed stiffness gave virtually identical peak impact load (differences of less than 1%).

To accurately represent the bridge pier's response to the vehicle impact load, it was deemed necessary to model the piles and the soil-pile interaction. A simple but effective method is used to model the lateral pile response. Beam elements are used to repre-

sent the piles and four discrete lateral spring elements are used to model the soil-pile interaction (Fig. 4). The springs are spaced at 660 mm for Pier I and at 440 mm for Pier II. The soil springs are modeled using inelastic bar elements that provide compression only response, since soil cannot provide any tensile resistance. The compressive stiffness of the springs was calculated using an approach discussed in El-Tawil (2004). The pier/bridge models are comprised of about 25,000 elements each.

Parametric Study and Naming Convention

The truck models are allowed to impact each pier in a head-on manner in two directions: (1) transverse to the longitudinal axis of the superstructure, and (2) parallel to the longitudinal axis of the bridge. These two directions are expected to have different structural characteristics because of the effect of the superstructure. The possibility of impact at other angles was not considered to reduce the computational effort. Based on extensive sensitivity studies, a coefficient of friction of 0.3 is assumed for both static and dynamic friction, and slight damping is imposed to reduce numerical problems. Numerical studies showed that the damping used had negligible influence on the computed peak forces. Each impact event is simulated using *LS-DYNA* (2002) for a period of 200 ms using a 1 μ s minimum time step. Various quantities of interest are extracted from the finite element results including: impact force versus time relationship, stress and strain values and rates at key points, pier deformations, pile forces, and pile deformations. Fig. 5 shows various views of the model and impact event involving the Chevy truck and Pier I. Fig. 6 shows a close-up of the Ford vehicle colliding with Pier II at various times. The figures clearly depict the severity of the crashes.

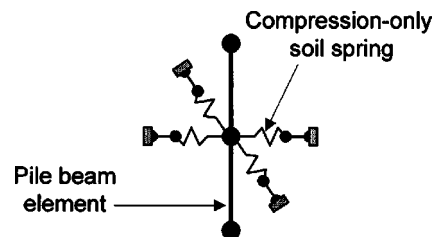


Fig. 4. Pile-soil interaction model

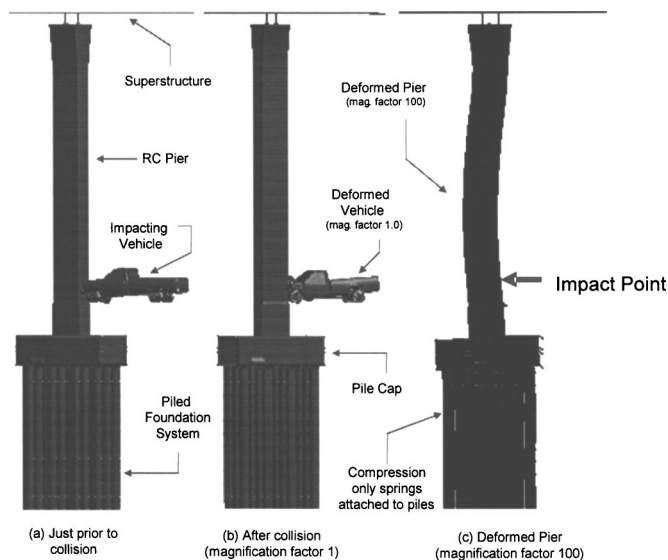


Fig. 5. Model representing impact simulation between the Chevy truck and Pier I

To simplify referral to the various runs conducted, each run is referred to by a unique descriptive name. For example, for the 14-kN Chevy truck traveling at 90 kph and impacting Pier I in the transverse direction (transverse to the longitudinal axis of the bridge), the run notation would be T14-V90-T-I. As another example, T66-V55-P-II represents the 66-kN Ford truck impacting Pier II in a direction parallel to the bridge axis at 55 kph.

Accuracy of Results

Zaouk et al. (1996) used the results of two collision tests to evaluate the accuracy of the Chevy model used in this research. The

first test involved a frontal 55-kph impact with a fully rigid wall, while the second involved a 100-kph, 25° glancing impact with a vertical concrete barrier. Overall, good agreement between analysis and test results was achieved, including good physical/pictorial correlation, as well as good comparison between measured and computed displacement, velocity, and acceleration at key points.

Extensive mesh refinement studies were conducted as part of this project to ensure that the pier meshes were adequate. In addition, conservation of energy checks were conducted for all runs. Conservation of energy implies that the initial kinetic energy of the vehicle must be completely transformed into residual kinetic energy, energy lost to friction, internal energy stored in the deforming vehicle components and pier members, and energy used up by the hourglass control algorithm for finite elements with reduced integration formulations.

Energy was indeed conserved in all runs indicating that numerical problems were not rampant, but hourglass energy in some of the initial runs was excessive and adversely affected confidence in the results of these runs. A large portion of the hourglass energy was expended in a few key parts in the vehicle models that are represented using reduced integration shell or solid elements. To remedy the hourglass energy situation, various vehicle components were either remeshed or were assigned fully integrated finite element formulations.

For each run, the percentage of hourglass energy at the instant of peak contact force and at rebound is listed in Table 1 for the Ford truck, and the evolution of various energy quantities is shown in Fig. 7 for run T66-V135-T-I. Rebound is defined as the instant when the resultant impact force drops to 1% of the peak value. At peak force, the hourglass energy ratio is quite low, but increases significantly to a maximum value at rebound. The results of the analyses were felt to be reasonable given that the hourglass energy ratio at peak load is so low, and that the maximum values are not excessively high. Zaouk et al. (1996) reported

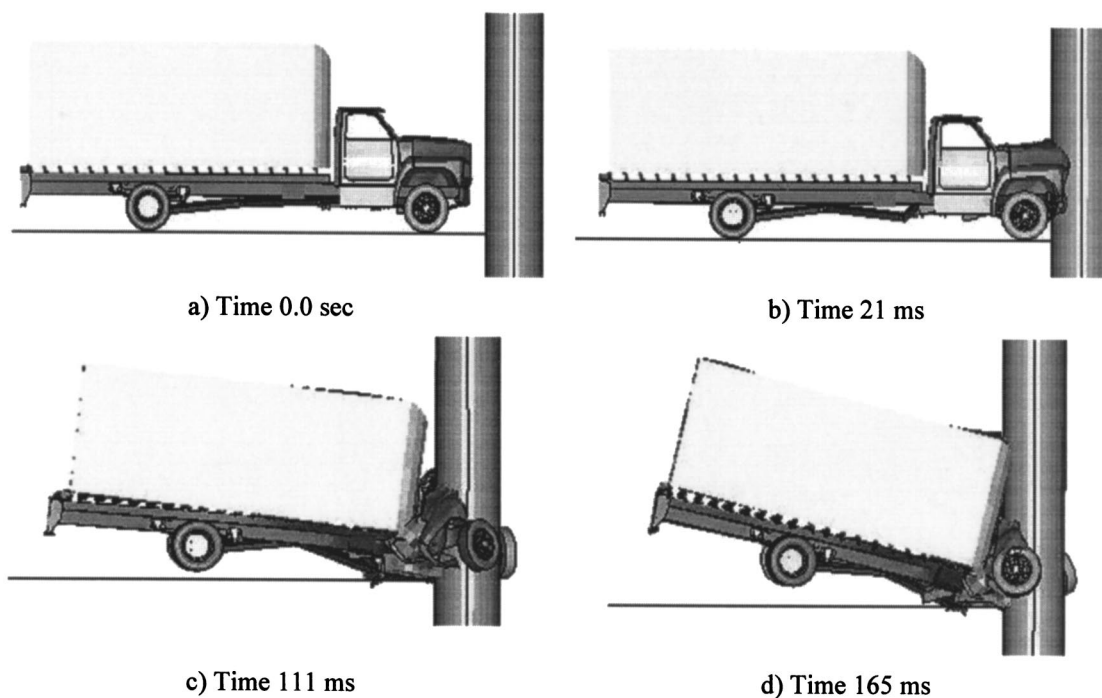


Fig. 6. Progression of collision between Ford Truck and Pier II for 110 kph approach speed

Table 1. Impact Force Measures and Hourglass Energy Ratio for Ford Truck

Run	PDF (kN)	ESF (kN)	Percent hourglass energy (at peak dynamic force)	Percent hourglass energy (at rebound)
T66-V55-T-I	5,180	2,150	6.2	10.2
T66-V90-T-I	16,200	4,800	2.5	9.2
T66-V110-T-I	17,800	6,450	2.3	14.2
T66-V135-T-I	26,300	8,850	2.0	16.9
T66-V55-T-II	5,160	2,450	2.6	6.8
T66-V90-T-II	7,600	3,700	1.4	9.0
T66-V110-T-II	11,300	4,800	1.0	11.3
T66-V135-T-II	17,700	6,650	1.0	12.2

Note: PDF=peak dynamic force; and ESF=equivalent static force.

17% hourglass energy at the end of their run in the head-on collision validation exercise, but deemed the results of their analysis acceptable.

To lend further credence to the analyses presented in this paper, albeit in a qualitative rather than quantitative manner, comparison between analysis and test results involving a truck crashing into a security bollard are presented (Albersen, private communication, 2003). The bollard dimensions were not provided for security reasons. The exact details of the truck are also not available; however, the truck weight is 66 kN, which is similar to the weight of the truck model used herein, and the approach speed is 78 kph. The simulation corresponding most closely to the bollard impact scenario is T66-V90-T-II, which is used for comparison. Comparison between the 10-ms average force versus time plots for both analysis and test is shown in Fig. 8. Given the large difference in structural properties between a bollard and Pier II as well as the different approach speeds (78 kph versus 90 kph), it is clear that the simulation captures the overall trend in a reasonable manner compared to the test. The peak force for T66-V90-T-II is 3,080 kN and the measured peak force is 2,350 kN (a difference of 31%).

Structural Demands and Force Measures

The force versus time responses generated by transverse impact of the Chevy truck for various approach speeds are shown in Figs.

9(a and b) for Piers I and II, respectively. A similar plot for the Ford truck approaching at 135 kph is also shown in Fig. 10. Several observations are evident from these two figures. The impact force versus time function appears to be comprised of a relatively low force level that is sustained over the duration of the impact event combined with several large spikes. The sharp spikes occur when stiff or heavy components of the vehicle, such as the chassis or engine block, reach the pier and interact with it. As the approach speed increases (Fig. 9), the first significant spike occurs earlier in time compared to slower approach speeds, which is expected.

Several force measures are used to characterize each impact event. The peak dynamic force (PDF) is the largest impact force computed during the simulation. The PDF usually occurs early on in a run as shown in Figs. 9 and 10. The PDF is not representative of the design structural demands that engineers need to consider because the structure has not had “time” to respond to the rapid change in loading. According to Chopra (2001), the equivalent static force (ESF) is a more appropriate measure of the design structural demand. The ESF is the static force necessary to produce the same deflection at the point of interest as produced by the dynamic event and is a function of the stiffness of the system and its dynamic characteristics. The peak 50 ms average (PFMA) force is also computed for comparison in the case of the Chevy truck. The definition of this quantity is rather arbitrary, but it has

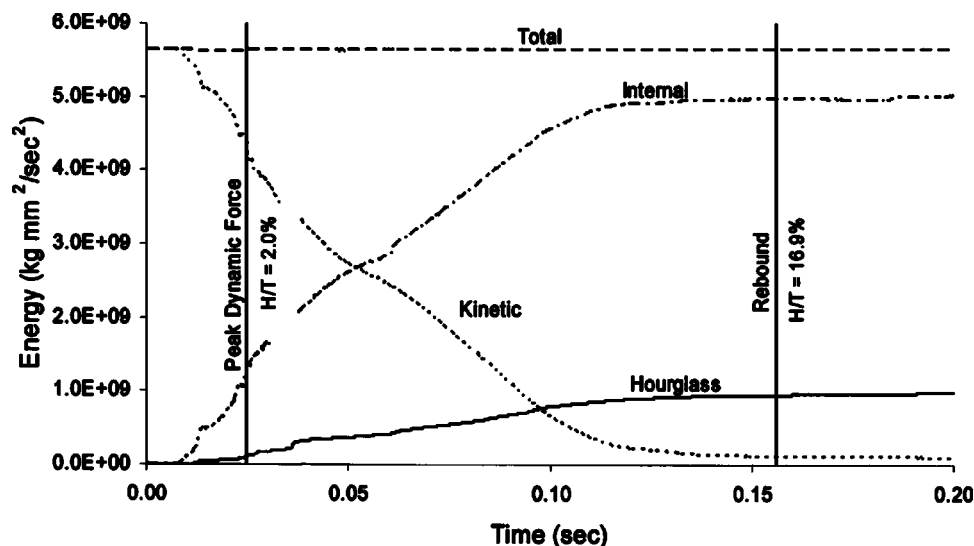


Fig. 7. Evolution of various energy quantities for T66-V135-T-I

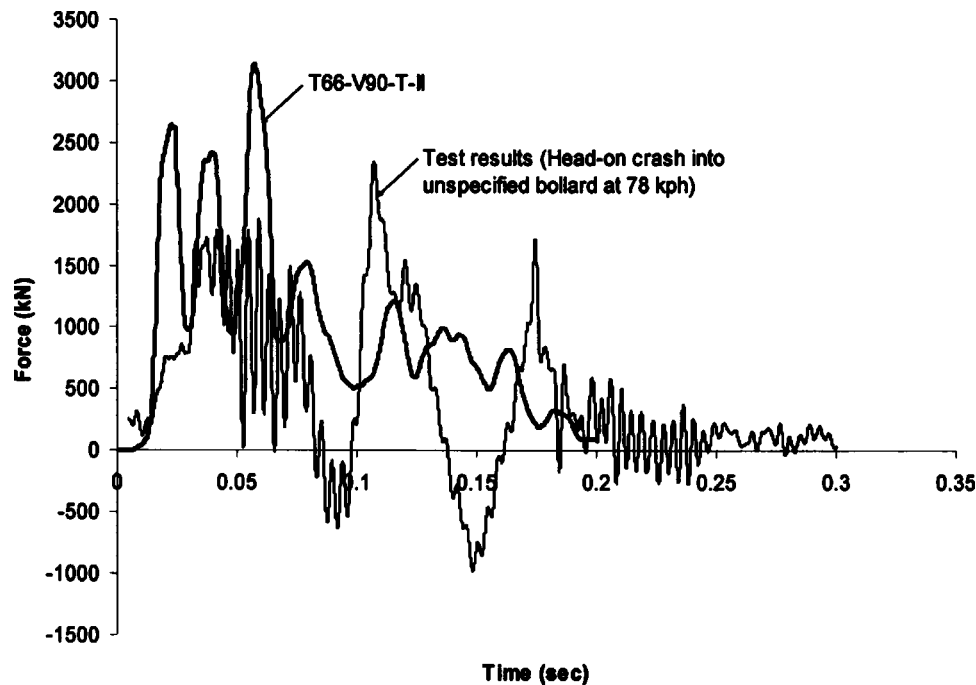


Fig. 8. Comparison between test results and comparable analysis T66-V90-T-II. Forces are average over 10-ms period

been frequently used by researchers in the automotive crash arena because it is simple to compute.

It was observed during the research that the PDF is quite dependent on the ratio of hourglass energy to the total energy in the system. In general the PDF grows as the ratio of hourglass energy grows. Fortunately, the ESF is not as sensitive to this modeling issue.

The PDF and ESF quantities are listed in Tables 1 and 2 for both trucks and plotted in Figs. 11 and 12 along with the AASHTO-LRFD design impact force (1,800 kN). Only quantities pertaining to transverse impact (i.e., transverse to the bridge axis) are presented. Parallel impact (i.e., travel parallel to the bridge axis) is rather unlikely, and in any case the forces generated by such a situation do not differ much from transverse impact. Data pertaining to impact parallel to the bridge axis is presented in

El-Tawil (2004). The PFMA values are computed for the Chevy truck runs and are listed in Table 2.

Analysis of Results

For the Chevy truck (Fig. 12), the peak dynamic forces (PDF) for both piers appear to increase almost linearly with increasing vehicle speed. This suggests that the impact process can be represented as an impulse. In impulse situations, assuming that the basic shape of the force versus time relationship remains relatively unchanged (which is the case for the Chevy impact as shown in Fig. 9), the peak impact force is a linear function of the momentum of the impacting body. However, the situation is not as simple for the Ford truck, where the PDF versus speed relation is not linear (Fig. 11).

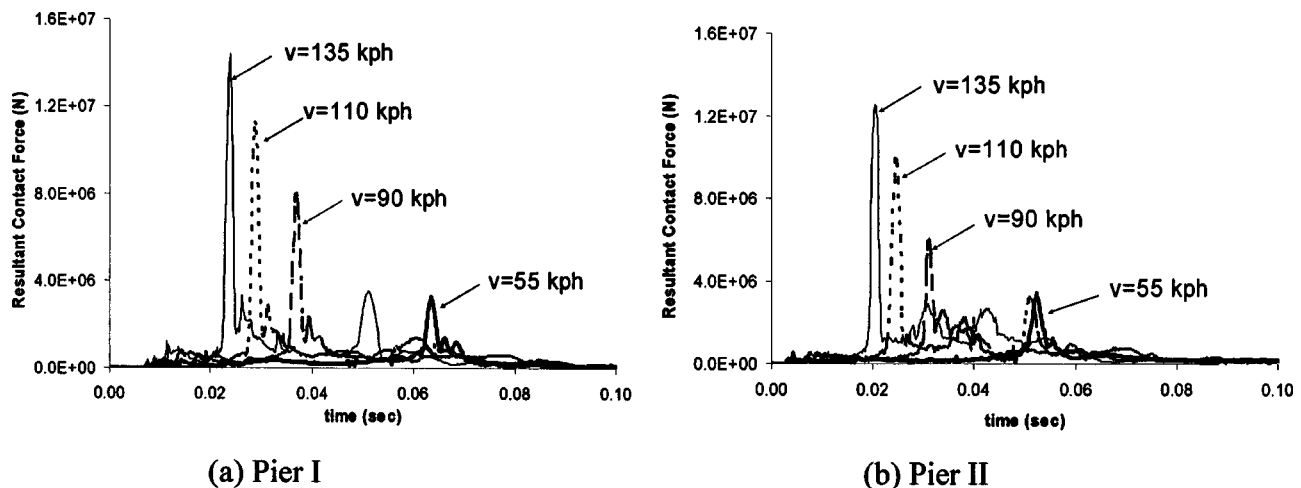


Fig. 9. Impact force versus time for Chevy truck at various speeds approaching in transverse direction

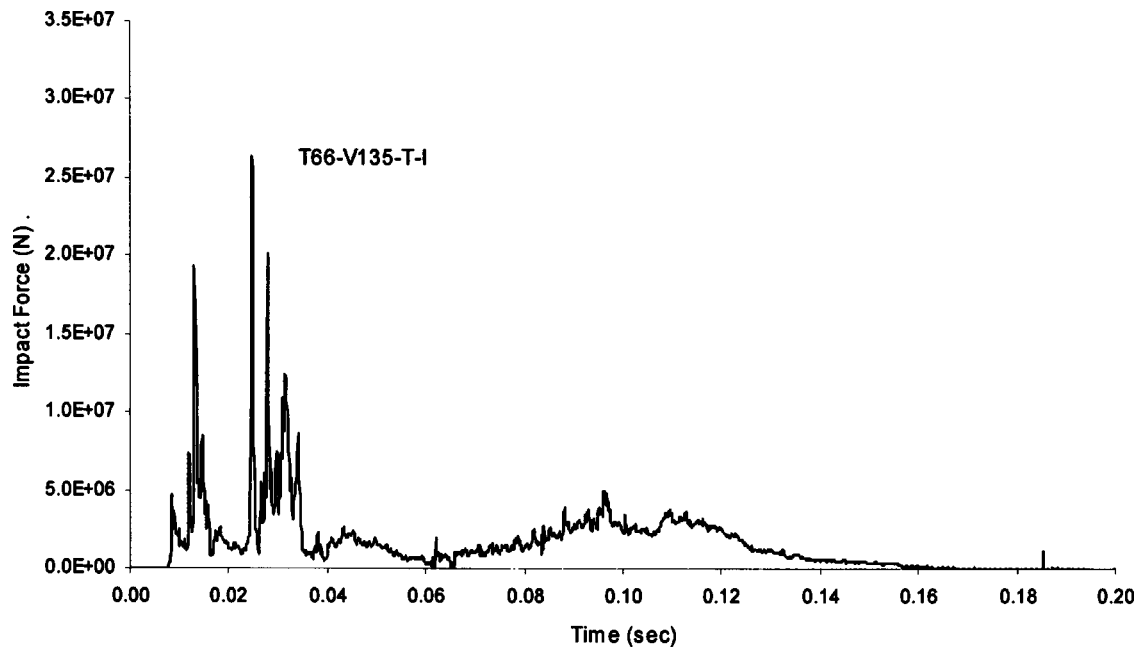


Fig. 10. Impact force versus time for Ford truck approaching Pier I at 135 kph in transverse direction

The ESF values for both trucks and both piers appear to have a linear relationship to the approach speed. The ESFs and PDFs are smaller for Pier II compared to Pier I. There are two reasons for this. First, Pier I is significantly stiffer at the point of impact compared to Pier II, and hence would attract greater force. Second, the large rectangular cross section of Pier I (1,450 × 1,375 mm) mobilizes more of the structural system of the impacting vehicle leading to greater collision forces than the smaller circular section (1,075 mm diameter) of Pier II. The only exception to this is case T66-V55-T-I, where the ESF is a little smaller (12% smaller) than the ESF for T66-V55-T-II. Although it is difficult to pinpoint a specific reason for this discrepancy given the complexity of the vehicle–pier interaction, one possible cause could be sensitivity to numerical problems. For example, from Table 1, it can be seen that the hourglass energy at peak force for T66-V55-T-I is significantly higher than for all other analysis cases.

The ESFs and PDFs for the Chevy truck are significantly less than the corresponding values for the Ford truck. This is expected given that the latter is about five times heavier than the former. However, it is interesting that the PDFs and ESFs for the Ford truck are less than five times their counterpart values for the

Chevy truck, implying that differences in the relative strength and stiffness of the structural system of both trucks are significant. In other words, the Ford truck is not able to deliver impact forces “as efficiently” as the Chevy truck.

As previously discussed, automotive crash researchers have used a 50-ms moving average to characterize impact force. The peak value (PFMA) is listed in Table 2 for the Chevy truck. It is clear that the PFMA does not correlate well with the ESF for Pier I. The ESF is a more logical measure of the force demand imposed on the pier, and is in fact the approach adopted by AASHTO-LRFD (1998).

Design Implications

For the Chevy truck (Fig. 12), the ESF is less than the AASHTO-LRFD design force for Pier II. It exceeds the AASHTO-LRFD design force for Pier I at approach speeds in excess of 80 kph. At the highest approach speed, the ESF for the Chevy truck is about 70% greater than the design impact force. For the Ford truck, the ESF is greater than the AASHTO-LRFD force for all approach speeds considered. At the highest speed, the ESF is significantly greater than the design force (4.9 times higher for Pier I).

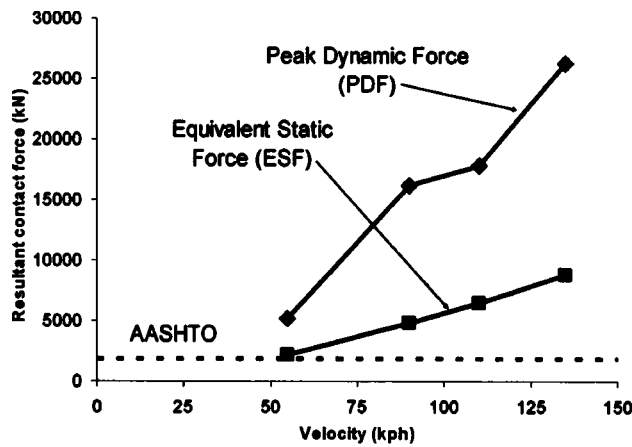
In evaluating the implications of these results it is important to understand the assumptions used to derive them. Although the vehicles as well as soil–pier interaction are modeled in an inelastic manner, the pier itself and the superstructure are modeled as elastic. Progressive collapse of the piers under the effect of impact cannot therefore be simulated using this model. However, the assumption of elastic pier behavior permits convenient definition of a design-oriented ESF, and therefore allows direct assessment of current design provisions. Given the high computed value of the ESF for some of the simulations, this research therefore suggests that current AASHTO-LRFD collision criteria could be deficient.

An examination of pier deformation profiles shows the top of the pier moves much less than the point of impact as a result of the inertial effect of the superstructure. Since there is substantial

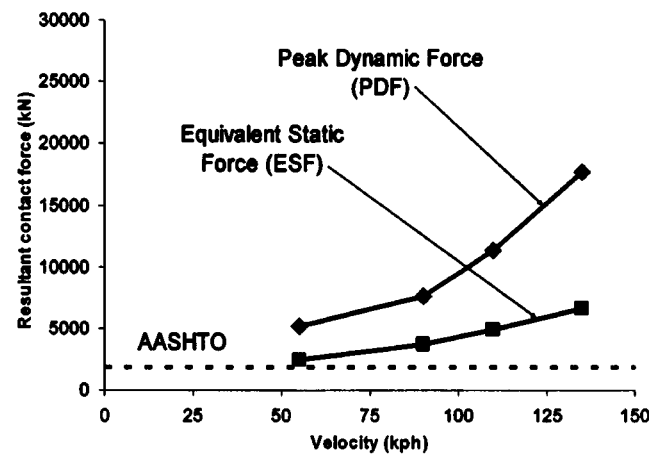
Table 2. Impact Force Measures for Chevy Truck

Run	PDF (kN)	ESF (kN)	PFMA (kN)
T14-V55-T-I	3,272	1,075	498
T14-V90-T-I	8,010	2,189	839
T14-V110-T-I	11,290	2,504	1,121
T14-V135-T-I	14,420	3,068	1,391
T14-V55-T-II	2,850	622	531
T14-V90-T-II	6,038	945	904
T14-V110-T-II	9,985	1,196	1,249
T14-V135-T-II	12,500	1,593	1,526

Note: PDF=peak dynamic force; ESF=equivalent static force; and PFMA=peak 50 ms average.



(a) Pier I



(b) Pier II

Fig. 11. Impact force versus approach speed relationship for Ford truck

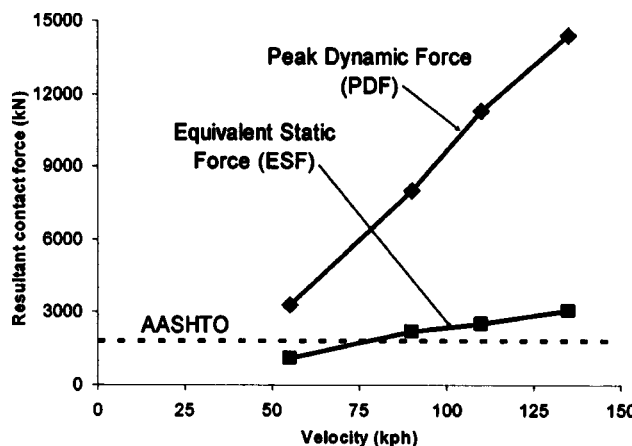
rotational restraint at the bottom of the pier because of the pile cap, it is therefore appropriate to quasi-statically model the pier as pinned at the top, fixed at the base with a concentrated ESF acting at the point of impact. Using such a model, it can be shown that the majority of the ESF acts as a shear force at the base of the pier (96% for Pier I and 91% for Pier II). Using ACI-318(ACI 2005), the shear capacity (without strength reduction factor and including the effect of column axial compression) of Piers I and II are 5,500 and 2,370 kN, respectively. These numbers imply that it is unlikely that the Chevy truck will cause shear failure of either pier at any of the approach speeds considered (compare 2,370 kN to ESF in Fig. 12 and Table 2). However, according to the simulations, the Ford truck can deliver ESFs in excess of the predicted shear capacity of Pier I for speeds greater than 100 kph, and Pier II for any of the considered speeds.

The recent failures presented in the "Introduction" are not proof that the AASHTO-LRFD collision provisions are deficient because it is unclear if the piers were designed for impact. It is also not known if the guard rails protecting the piers meet current crashworthiness criteria. Nevertheless, together with the discussions presented above, these failure events indicate that there

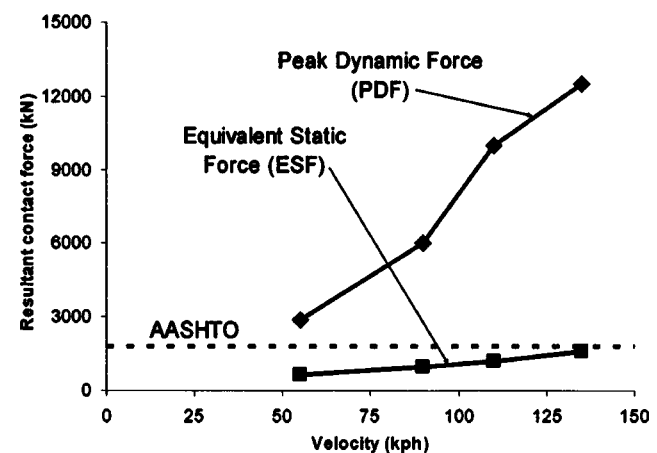
could be a population of bridge piers that are vulnerable to accidental or malevolent impact by heavy trucks.

Concluding Remarks and Ongoing Work

An investigation into the impact behavior of bridge piers has been presented. Two publicly available truck models were considered, a 14-kN Chevy truck (representing light trucks) and a 66-kN Ford truck (representing medium weight trucks). The truck models were crashed into finite element models of two different bridge piers, and the peak dynamic forces and corresponding equivalent static forces were calculated. Although physical vehicle-pier impact tests were not carried out to verify the accuracy of the simulations, a variety of exercises were conducted to provide confidence in the analysis results. These exercises included: reviewing previously published verification studies involving the 14-kN truck, mesh refinement studies, energy balance audits, monitoring of hourglass control energy during the simulations, and comparison of pertinent results to data from truck/bollard collision tests.



(a) Pier I



(b) Pier II

Fig. 12. Impact force versus approach speed relationship for Chevy truck

The results of the simulations showed that, in general, the peak transient forces are very high, much higher than the AASHTO-LRFD collision design force. However, since the peak forces act for a short duration, equivalent static forces were computed to serve as a measure of “design” structural demands during collision. The computed equivalent static forces turned out to be significantly higher than the AASHTO-LRFD design force for a number of simulations.

These results imply that the AASHTO-LRFD design provisions could be unconservative for feasible crash scenarios such as those considered herein. This is disturbing because heavier trucks, such as tractor-trailers, could generate even higher demands. It is furthermore troublesome that there are no guidelines on how to detail a vulnerable member to ensure that it will survive (with a specific structural performance in mind) a catastrophic impact situation.

The simulations presented in this paper demonstrate that numerical modeling of this sort could serve as a powerful tool to investigate the vulnerability of specific bridges or to improve general design criteria. The writers are currently continuing this research by refining some of the assumptions involved, e.g., modeling the inelastic behavior of the concrete and reinforcement in the piers, using various other vehicles as impactors, and developing design oriented criteria suitable for implementation in specifications.

Acknowledgments

Financial support for this research was provided in part by the Florida Department of Transportation (Project BC-355-6), the National Science Foundation (Project 0334364), and the University of Michigan. The writers are grateful to Dr. Dean Alberson of TTI and Mr. Don Moffett at the Department of State for providing the vehicle/bollard collision data. The opinions stated here are those

of the writers and do not necessarily reflect the views of the sponsors or the individuals mentioned above.

References

- American Association of State Highway and Transportation Officials Load and Resistance Factor Design (AASHTO-LRFD). (1998). *LRFD bridge design specifications—Second edition*, AASHTO, Washington, D.C.
- American Concrete Institute (ACI). (2005). *Building code requirements for structural concrete (318-05) and commentary (318R-05)*, ACI, Farmington Hills, Mich.
- Chopra, A. K. (2001). *Dynamic of structures: Theory and applications to earthquake engineering*, 2nd Ed., Prentice-Hall, Englewood Cliffs, N.J., 2001.
- Dallas-News. (2002). <http://www.dallasnews.com/latestnews/stories/090802dnmetrichland.1368b84.html>.
- El-Tawil, S. (2004). “Vehicle collision with bridge piers.” *Final Report to the Florida Department of Transportation for Project BC-355-6*, FDOT/FHWA publication.
- LS-DYNA; *theory manual for version 960*. (2002). Livermore Software Technology Corporation.
- Miyamoto, A., King, M. W., and Bulson, P. S. (1994). “Modeling of impact load characteristics for dynamic response analysis of concrete structures.” *Structures under shock and impact II*, Computational Mechanics Publications, Southampton, Boston, 71–88.
- National Transportation Safety Board (NTSB). (1993). “Tractor-semitrailer collision with bridge columns on Interstate 65 Evergreen Alabama.” *Highway accident report, NTSB Number HAR-94-2, NTIS Number PB94-916202*.
- “Nebraska overpass will be rebuilt with fewer piers.” (2003). *Engineering News Record*, June 9, 25.
- Roeder, C. W., Stanton, J. F., and Taylor, A. W. (1987). “Performance of elastomeric bearings.” *National Cooperative Highway Research Program Report 298*, Transportation Research Board, Washington, D.C.
- Zaouk, A. K., Bedewi, N. E., Kan, C. D., and Marzoughi, D. (1996). “Validation of a non-linear finite element vehicle model using multiple impact data.” *Crashworthiness and occupant protection in transportation systems*, AMD-Vol. 218, ASME, New York, 91–106.